American Mineralogist, Volume 68, pages 164–176, 1983

Composition, order–disorder and lattice parameters of olivines: relationships in silicate, germanate, beryllate, phosphate and borate olivines

GREGORY R. LUMPKIN

Department of Physics
University of California
Berkeley, California 94720

AND PAUL H. RIBBE

Department of Geological Sciences
Virginia Polytechnic Institute and State University
Blacksburg, Virginia 24061

Abstract

A general formula for olivine-type compounds is $(M1)(M2)TO_4$, where M1 and M2 represent octahedrally coordinated cations and T is the cation tetrahedrally coordinated by oxygen. Using 52 natural and synthetic olivines with known crystal structures, with M1 and M2 variously Li, Na, Mg, Al, Ca, Sc, Cr, Mn, Fe, Co, Ni, Zn, Ga, Y, Cd, Sm, Gd, and Lu, and with T = Be, B, Si, P, Ge, or (Si_xGe_{1-x}), we have quantified and analyzed the relationships among lattice parameters, effective ionic radii (r_{M1},r_{M2},r_T) and charge on the cations (q_{M1},q_{M2}; $q_T = 8.0 - q_{M1} - q_{M2}$) using multiple linear regression techniques. Of the regression equations listed below, only that for the *a* cell dimension was significantly improved (to $R^2 = 0.99$) by the inclusion of q terms (see text).

$$a = 1.096\ r_{M1} + 0.330\ r_{M2} + 1.105 r_T + 3.419\ \text{Å};\ R^2 = 0.970$$
$$b = 0.662\ r_{M1} + 3.305\ r_{M2} + 0.982 r_T + 7.061\ \text{Å};\ R^2 = 0.990$$
$$c = 1.045\ r_{M1} + 1.623\ r_{M2} + 0.651 r_T + 3.859\ \text{Å};\ R^2 = 0.991$$
$$V = 142.7\ r_{M1} + 197.7\ r_{M2} + 147.9 r_T + 4.703\ \text{Å}^3;\ R^2 = 0.997$$

Similar and more precise sets of equations were calculated separately for silicate, phosphate and beryllate olivines. The utility of these equations for predicting whether a particular structure has an ordered, disordered or antiordered (large cation in M1) distribution of octahedral cations has been successfully tested, especially in cases where $|r_{M1} - r_{M2}| > 0.1$Å, and a technique is suggested for predicting both the bulk composition and the cation distribution using only the *a* and *b* cell dimensions.

Introduction

A large number of compounds crystallize with the olivine structure, variously symbolized M_2TX_4 or A_2BX_4, where M (= A) represents octahedrally coordinated cations, T (= B) represents tetrahedrally coordinated cations, and X represents the four-coordinated anions, which usually are oxygen but also may be fluorine, sulfur or selenium.

In nature, by far the most important rock-forming olivines are members of the forsterite–fayalite series, $(Mg,Fe)_2SiO_4$, which often contain minor amounts of other divalent substituents, notably Ca, Mn, and Zn, with occasional traces of Ni. Other natural silicate olivines contain these same divalent cations in various proportions as *major* constituents. Brown (1970, 1980) has studied the crystal chemistry of the natural silicate olivines in great detail. We will incorporate some of his results in this investigation, as well as those for several nonsilicate minerals with the olivine structure: chrysoberyl (Al_2BeO_4), sinhalite ($AlMgBO_4$) and rare phosphates with charge-balancing combinations of $(Na,Li)^{1+}$ and $(Mg,Fe,Mn)^{2+}$ as the principal octahedral cations. Adding to our data base are a great many M_2TO_4 compounds (with T = Be, B, Si, P, S, Cl, Ge, As, Se) which have been synthesized (*cf.* Ganguli, 1977).

We have selected a variety of both synthetic and natural beryllates, borates, silicates, phosphates,

0003–004X/83/0102–0164$02.00

germanates, and germano-silicates for our study, in which we attempt to quantify by multiple linear regression analysis the relationships among lattice parameters, the mean radii of cations occupying the tetrahedral site (T) and the two distinct octahedral sites (M1 and M2), and the formal charges of the cations in these sites. The usefulness of this procedure has been demonstrated in studies of *C2/c* pyroxenes (Ribbe and Prunier, 1977), silicate garnets (Novak and Gibbs, 1971), and compounds with the spinel structure (Hill *et al.*, 1979). Significant results for olivines are interpreted in structural terms and are used for prediction of composition and ordering in other compounds with the olivine structure. Ganguli's (1977) attempts to do this, consisting of simple plots of *a*, *b*, and *c vs.* mean radii of the M1 and M2 octahedral cations for silicate and germanate olivines, resulted in some misleading conclusions.

Description of the olivine structure

M_2TX_4 compounds crystallizing with the olivine structure are characterized by hexagonal closest packed arrays of X anions in which one-half of the octahedral interstices are occupied by M cations, and one-eighth of the tetrahedral interstices are occupied by T cations. The idealized polyhedral drawings of Sung and Burns (1978) show the corner- and edge-sharing octahedra and tetrahedra in the olivine structure (Fig. 1, and see Fig. 1 in Brown's (1980) review). Conventionally, the major structural features have been considered to be the zigzag chains of occupied M1 and M2 octahedra, parallel to *c*, which are cross-linked to other such parallel chains in the (100) plane by corner-sharing T tetrahedra (Fig. 1a). When certain empty tetrahedral sites (the "leer" tetrahedra of Hanke (1965), designated L after Sung and Burns (1978)) are considered, a series of L–T chains oriented parallel to *a* (Kamb, 1968) become evident in Figures 1b and 1c. Then one may call attention to other structural units such as the M1–T,L slabs oriented parallel to (010) (Fig. 1b), and the linkage of these slabs by M2 octahedra in the (001) plane (Fig. 1c). The M2 octahedra accomplish the linkage through edge sharing with two M1 octahedra and one tetrahedron in one slab, and corner sharing with three tetrahedra in the adjacent M1–T,L slab (Fig. 1a,c).

Predicted lattice parameter variations

Since this study is concerned only with O-bearing olivines, the first-order effects on the cell dimensions of these olivine-type compounds will be limited to the effective radii of the cations and their electrostatic interactions.

Size effects of cation substitutions. With reference to Figures 1a and 1c, one might expect the *a* cell dimension to be directly affected by variations in the radii, r_{M1} and r_T, of the M1 and T cations. The *b* dimension should be sensitive primarily to the mean effective radius, r_{M2}, of the cations occupying M2 octahedra (Figs. 1a and 1c) whereas the *c* dimension, which is parallel to the edge-sharing –M1–M1–M1– spine of the zigzag octahedral chain (Fig. 1a) presumably would be most affected by the mean radius of the cations occupying the M1 octahedra. Since there is, in effect, an additional "chain" of corner-sharing M2 and T polyhedra parallel to *c*, one must not underestimate the combined effects of r_{M2} and r_T on the *c*-dimension. Unit cell volume will be a function of the mean effective radii of all constituent cations.

Effects of formal charges of M and T cations. The effects of cation–cation repulsion on bond angles and interatomic distances have been systematically studied for M^{2+} olivines (Brown, 1970, 1980, p. 316) and the related, homologous series of humite minerals (Ribbe, 1980, p. 248) in terms of Pauling's (1929) third rule. However, the effects of inter-cation repulsions on lattice parameters have not been

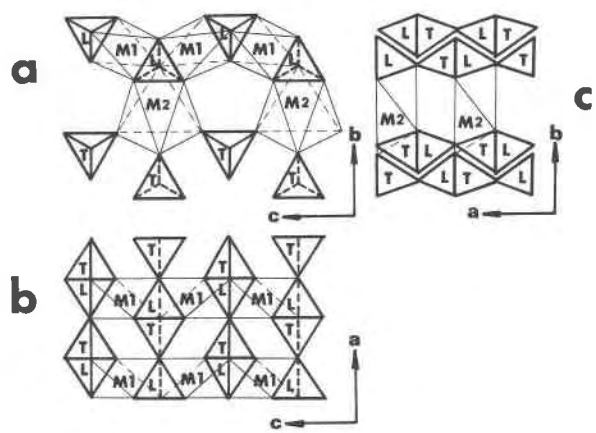

Fig. 1. Polyhedral drawings of the olivine structure. (a) Projection down the *a* axis showing edge-sharing between the M1 and M2 octahedra in the M1–M2 zigzag chain running parallel to *c*, and corner sharing between the M2 and T sites. T = occupied tetrahedron; L = "leer" or unoccupied tetrahedron. (b) This projection down the *b* axis shows the framework of M1 and T and L tetrahedral sites parallel to (010), referred to as M1-T,L slabs in the text. (c) The *c* axis projection clearly shows, along with (a), how the M1–T,L slabs parallel to (010) are linked together by the M2 octahedra. From Sung and Burns (1978, Fig. 5, p. 184); used by permission of Springer-Verlag.

investigated, and with good reason. The "size" (effective ionic radius) of a cation is largely governed by its outer electron configuration so that cation size and charge are intimately linked: to attempt to differentiate their effects on unit cell dimensions is difficult without the use of multiple regression techniques. Some effect of charge interaction on the *a* and *c* lattice parameters might be expected, because (i) the M1 · · · T distance is the shortest of the interaction distances, (ii) there are twice as many short M1 · · · T repulsion terms in olivines because the M1 octahedron shares twice as many edges with T tetrahedra as the M2 octahedron does, and (iii) the major components of the M1 · · · T repulsions are in the (010) plane (see Fig. 1b).

We shall discover that for the known cation distributions in olivines, (Table 1), the contribution of formal charge terms in multiple regression equations is in fact relatively inconsequential. However, the effects of charge cannot be ignored in rationalizing the cation distributions (ordering schemes) themselves, as Ganguli (1977) and others have discussed (*cf.* Alberti and Vezzalini, 1978). Of course, the ordering schemes have considerable influence on the lattice parameters, and for that reason we review the principles governing them in somewhat broader terms than Brown (1980, p. 334f.) who considered only the $M1^{2+}M2^{2+}$ silicates, and in somewhat different terms thán Ganguli (1977, p. 310f.), whose summary requires revision.

Rationalizations of cation ordering in M1,M2 octahedra

In addition to those mentioned in (i–iii) above, there are several observations basic to an understanding of $(M1)(M2)TO_4$ compounds with the olivine structure.

(1) Except for *traces* of Ti^{4+}, Cr^{3+} and Fe^{3+} (Shinno, 1981) in $M1^{2+}M2^{2+}$ natural olivines (Smith, 1966), there is no evidence that cations of different formal valences mix on a given octahedral site (see Table 1 and *cf.* Tables 5 and A3 in Brown (1980); Alberti and Vezzalini (1978) came to the same conclusion based on Madelung energy calculations).

In olivines containing only one species and oxidation state of cation in *both* octahedral sites (*e.g.*, Mg_2SiO_4, Al_2BeO_4), the M1 site is inherently 0.03–0.05Å smaller than the M2 site, using mean M–O bond lengths as a gauge of "size." The M1 octahedron is also slightly more distorted than M2, even at high temperatures. The size and distortion differences arise from the fact that the M1 octahedron has twice as many shared edges as M2. Thus, in general:

(2a) If valences and electronegativities are alike, smaller cations "prefer" M1, larger cations "prefer" M2. (2b) If cation sizes and valences are alike, the more electronegative element will prefer the smaller M1 octahedron because it permits a greater degree of covalent bonding (*e.g.*, Zn^{2+} over Mg^{2+}—Ghose *et al.*, 1975). (2c) If sizes and valences are alike, the transition metal cations, Cr^{3+}, Fe^{2+}, Co^{2+}, and Ni^{2+} prefer the smaller and more distorted M1 site because in it they gain crystal field stabilization energy (CFSE) relative to M2.

The following is a restatement of conclusions (i)–(iii) from the previous section, in the terms of Moore (1972, p. 1340).

(3) "For cations of different charge but smaller crystal radius in an identical anionic matrix, the high-charged cation will favor the site with the minimum overall nearest neighbor cation–cation repulsion." In other words, in $NaMnPO_4$ (natrophyllite), the large Na^{1+} cation "prefers" M1, the smaller but more highly charged Mn^{2+} "prefers" M2, and this compound is completely *antiordered* (which means that the larger cation is entirely concentrated in M1), in accord with principle (1) above.[1]

The well-documented crystal chemical principles presented in (2a,b,c) and (3) "compete" with one another in the sense that is illustrated in the $(Mg, Fe)_2SiO_4$ solid solution series. CFSE causes Fe^{2+} to "prefer" M1, but its slightly larger size causes it to prefer M2. Crystallization and annealing conditions for synthetic compounds and overall paragenesis for natural olivines are important, too. For example, many Mg,Fe olivines are disordered, in a few Fe^{2+} prefers M2 (Wenk and Raymond, 1973) though most contain more Fe^{2+} in M1 than in M2 (up to 20% more in a lunar sample—Virgo and Hafner, 1972).

The purpose of this paper and a following paper is not only to develop a quantitative understanding of the variation of lattice parameters of olivine-type compounds as a function of cation size and charge,

[1]Moore's principle is violated in sinhalite, $AlMgBO_4$ (Fang and Newnham, 1965): the smaller, more highly charged Al^{3+} (r = 0.535Å) is in the smaller M1 site and Mg^{2+} (r = 0.72Å) is in the M2 site consonant with the greater covalence of Al. Since there are equal numbers of divalent and trivalent cations, sinhalite is completely ordered (*cf.* principle 1).

Table 1. Octahedral cation distributions in M1 and M2 sites, mean cation radii r_{M1} and r_{M2}, formal charges q_{M1} and q_{M2}, and lattice parameters of silicate, germanate, beryllate, phosphate, borate, and germanosilicate olivines whose crystal structures have been refined. References are listed at the end of this table. Units in Å, except volume (Å^3) and q (e.s.u.).

Ref.	(M1)	r_{M1}	q_{M1}	M2	r_{M2}	q_{M2}	*a*	*b*	*c*	V	
				SILICATES (r_T = 0.260)							
1	(Ni)	0.690	2	Ni	0.690	2	4.726	10.118	5.913	282.8	
2	($Ni_{.77}Mg_{.23}$)	.697	2	$Ni_{.26}Mg_{.74}$	.712	2	4.740	10.170	5.940	286.3	
3	(Mg)	.720	2	Mg	.720	2	4.756	10.207	5.980	290.3	
4	($Mg_{.73}Zn_{.27}$)	.725	2	$Mg_{.84}Zn_{.16}$	.723	2	4.774	10.234	5.997	293.0	
5	($Mg_{.81}Fe_{.19}$)	.731	2	$Mg_{.83}Fe_{.17}$	.730	2	4.771	10.274	6.011	294.6	
6	(Mg)	.720	2	$Mg_{.91}Ca_{.09}$	.745	2	4.761	10.250	6.002	292.9	
7	($Co_{.73}Mg_{.27}$)	.738	2	$Mg_{.63}Co_{.37}$	.729	2	4.775	10.258	5.996	293.7	
5	($Mg_{.68}Fe_{.32}$)	.739	2	$Mg_{.21}Fe_{.29}$	.737	2	4.785	10.298	6.028	297.0	
8	(Co)	.745	2	Co	.745	2	4.781	10.300	6.004	295.5	
6	(Mg)	.720	2	$Mg_{.82}Ca_{.18}$	.770	2	4.769	10.318	6.035	297.0	
9	(Li)	.760	1	Sc	.745	3	4.819	10.436	5.969	300.0	
3	($Fe_{.56}Mg_{.36}Mn_{.08}$)	.762	2	$Fe_{.54}Mg_{.39}Mn_{.07}$	.760	2	4.798	10.387	6.055	301.8	
4	($Mg_{.72}Mn_{.28}$)	.751	2	$Mn_{.66}Mg_{.34}$	.793	2	4.811	10.421	6.116	306.6	
10	($Mg_{.92}Mn_{.08}$)	.729	2	$Mn_{.89}Mg_{.11}$	.818	2	4.794	10.491	6.123	307.9	
11	(Fe)	.780	2	Fe	.780	2	4.818	10.470	6.086	307.0	
5	($Mg_{.71}Fe_{.29}$)	.737	2	$Mg_{.71}Fe_{.29}$	.737	2	4.775	10.280	6.016	295.3	
12	($Mn_{.43}Mg_{.35}Zn_{.18}Fe_{.04}$)	.773	2	$Mn_{.87}Fe_{.08}Zn_{.05}$	.822	2	4.833	10.567	6.173	315.3	
12	($Fe_{.66}Mn_{.29}Mg_{.05}$)	.792	2	$Mn_{.63}Fe_{.37}$	.812	2	4.844	10.577	6.146	314.9	
10	($Mn_{.83}Mg_{.17}$)	.811	2	Mn	.830	2	4.879	10.589	6.234	322.1	
13	(Mn)	.830	2	Mn	.830	2	4.901	10.598	6.257	325.0	
6	(Mg)	.720	2	$Ca_{.78}Mg_{.22}$	.938	2	4.814	10.913	6.292	330.6	
14	(Li)	.760	1	Y	.900	3	4.96	10.68	6.29	333.2	
6	(Mg)	.720	2	$Ca_{.89}Mg_{.11}$	.969	2	4.818	11.007	6.333	335.8	
15	(Mg)	.720	2	Ca	1.000	2	4.822	11.108	6.382	341.8	
1	($Mg_{.93}Fe_{.07}$)	.724	2	Ca	1.000	2	4.825	11.111	6.383	342.2	
16	(Co)	.745	2	Ca	1.000	2	4.827	11.12	6.422	344.7	
17	(Fe)	.780	2	Ca	1.000	2	4.910	11.126	6.457	352.7	
12	($Fe_{.85}Ca_{.15}$)	.813	2	$Ca_{.98}Fe_{.02}$	.995	2	4.892	11.180	6.469	353.8	
1	($Mn_{.85}Mg_{.10}Zn_{.05}$)	.815	2	$Ca_{.98}Mn_{.02}$	.997	2	4.913	11.151	6.488	355.4	
18	(Mn)	.830	2	Ca	1.000	2	4.944	11.19	6.529	361.2	
19	(Ca)	1.000	2	Ca	1.000	2	5.078	11.225	6.760	385.3	
14	(Na)	1.020	1	Lu	.861	3	5.09	11.00	6.33	354.4	*
				GERMANATES (r_T = 0.390)							
13	(Mg)	0.720	2	Mg	0.720	2	4.913	10.304	6.032	305.4	
13	(Mn)	.830	2	Mn	.830	2	5.04	10.70	6.26	337.6	
14	(Li)	.760	1	Y	.900	3	5.08	11.05	6.30	353.6	
30	(Mg)	.720	2	Ca	1.000	2	4.93	11.18	6.58	362.7	
13	(Cd)	.950	2	Cd	.950	2	5.200	11.147	6.572	380.9	
31	(Ca)	1.000	2	Ca	1.000	2	5.240	11.400	6.790	405.6	
33	(Mg)	.720	2	Mn	.830	2	4.982	10.559	6.181	325.2	*
33	(Co)	.745	2	Mn	.830	2	4.991	10.649	6.195	329.3	*
33	(Fe)	.780	2	Mn	.830	2	5.010	10.641	6.210	331.1	*
34	(Zn)	.740	2	Mn	.830	2	5.03	10.76	6.30	341.0	*
14	(Na)	1.020	1	Y	.900	3	5.17	11.28	6.42	374.4	*
14	(Na)	1.020	1	Lu	.861	3	5.20	11.22	6.32	368.7	*
14	(Na)	1.020	1	Gd	.938	3	5.25	11.49	6.50	392.1	*
14	(Na)	1.020	1	Sm	.958	3	5.28	11.53	6.55	398.8	*

Table 1. (continued)

Ref.	(M1)	r_{M1}	q_{M1}	M2	r_{M2}	q_{M2}	a	b	c	V	
				BERYLLONATES (r_T = 0.270)							
26	(Al)	0.535	3	Al	0.535	3	4.427	9.404	5.476	228.0	
27	($Al_{.95}Fe_{.05}$)	.541	3	$Al_{.85}Fe_{.15}$	.552	3	4.455	9.475	5.510	232.6	
27	($Al_{.96}Fe_{.04}$)	.539	3	$Al_{.64}Fe_{.36}$	.575	3	4.460	9.535	5.530	235.2	
27	($Al_{.91}Fe_{.09}$)	.545	3	$Al_{.49}Fe_{.51}$	.591	3	4.465	9.575	5.565	237.9	
27	($Al_{.93}Fe_{.07}$)	.543	3	$Al_{.27}Fe_{.73}$	.615	3	4.470	9.630	5.580	240.2	
28	(Al)	.535	3	Fe	.645	3	4.49	9.68	5.61	243.8	
29	(Cr)	.615	3	Cr	.615	3	4.555	9.792	5.663	252.6	
28	(Al)	.535	3	Cr	.615	3	4.51	9.73	5.62	246.6	*
28	(Al)	.535	3	Ga	.620	3	4.48	9.59	5.56	238.9	*
				PHOSPHATES (r_T = 0.170)							
20	(Li)	0.760	1	Ni	0.690	2	4.68	10.03	5.85	274.6	*
20	(Li)	.760	1	Mg	.720	2	4.68	10.15	5.87	278.8	*
20	(Li)	.760	1	Co	.745	2	4.70	10.20	5.92	283.8	*
21	(Li)	.760	1	Fe	.780	2	4.693	10.334	6.010	291.5	
22	(Li)	.760	1	$Fe_{.76}Mn_{.24}$	.792	2	4.703	10.359	6.029	293.7	
23	(Li)	.760	1	Mn	.830	2	4.744	10.460	6.100	302.7	
24	(Na)	1.020	1	$Mn_{.93}Fe_{.07}$	.827	2	4.987	10.523	6.312	331.2	
25	(Na)	1.020	1	Cd	.950	2	5.055	10.832	6.494	355.6	*
				BORATES (r_T = 0.110)							
32	(Al)	0.535	3	Mg	0.720	2	4.335	9.874	5.671	242.7	
				GERMANO-SILICATES (r_T = 0.293 for $Ge_{.25}Si_{.75}$, 0.325 for $Ge_{.50}Si_{.50}$ and 0.358 for $Ge_{.75}Si_{.25}$)							
31	(Ca)	1.000	2	Ca	1.000	2	5.124	11.260	6.767	390.4	
31	(Ca)	1.000	2	Ca	1.000	2	5.165	11.320	6.778	396.3	
31	(Ca)	1.000	2	Ca	1.000	2	5.201	11.362	6.781	400.7	

* Not used in regression analyses of Table 3. These are the test samples plotted in Figure 7.

REFERENCES:

1 Lager & Meagher (1978) Am. Mineral. 63, 365.
2 Rajamani *et al.* (1975) Am. Mineral. 60, 292.
3 Smyth & Hazen (1973) Am. Mineral. 58, 588.
4 Ghose *et al.* (1976) Acta Crystallogr. A31, S3, S76.
5 Brown & Prewitt (1973) Am. Mineral. 58, 577.
6 Warner & Luth (1973) Am. Mineral. 58, 998.
7 Ghose & Wan (1974) Contr. Mineral. Petrol. 47, 131.
8 Morimoto *et al.* (1974) Am. Mineral. 59, 475.
9 Ito (1977) Am. Mineral. 62, 356.
10 Francis & Ribbe (1980) Am. Mineral. 65, 1263.
11 Hazen (1977) Am. Mineral. 62, 286.
12 Brown (1980) Reviews in Mineralogy 5, 275.
13 Muller & Roy (1974) The Major Ternary Structural Families.
14 Blasse & Bril (1967) J. Inorg. Nucl. Chem. 29, 2231.
15 Onken (1965) Tschermaks Mineral. Petrogr. Mitt. 10, 34.
16 Newnham *et al.* (1966) J. Am. Ceram. Soc. 49, 284.
17 Wyderko & Mazanek (1968) Mineral. Mag. 36, 955.
18 Caron *et al.* (1965) J. Phys. Chem. Solids 26, 927.
19 Czaya (1971) Acta Crystallogr. B27, 848.
20 Newnham & Redman (1965) J. Am. Ceram. Soc. 48, 547.
21 Yakubovich *et al.* (1978) Sov. Phys. (Dokl.) 22, 347.
22 Finger & Rapp (1970) Carnegie Inst. Wash. Year Book 68, 290.
23 Geller & Durand (1960) Acta Crystallogr. 13, 325.
24 Moore (1972) Am. Mineral. 57, 1333.
25 Ivanov *et al.* (1974) Sov. Phys. Crystallogr. 19, 96.
26 Farrell *et al.* (1963) Am. Mineral. 48, 804.
27 Newnham *et al.* (1964) Am. Mineral. 49, 427.
28 Gjessing *et al.* (1943) Norsk. Geol. Tidsskr. 22, 92.
29 Weir & van Valkenburg (1960) J. Res. Nat. Bur. Stand. A64, 103.
30 Strunz & Jacob (1960) N. Jahrb. Mineral. Abh., 78.
31 Eysel & Hahn (1970) Z. Kristallogr. 131, 322.
32 Claringbull & Hey (1952) Mineral. Mag. 29, 841.
33 Ringwood & Reid (1970) J. Phys. Chem. Solids 31, 271.
34 Lyutin *et al.* (1974) Sov. Phys. (Dokl.) 19, 10.

but also to provide a basis for predicting whether a given olivine is ordered, disordered or antiordered, and if disordered, to what extent.

Data acquisition and procedures

The lattice parameters, composition, and site distribution of cations from 52 natural and synthetic compounds with the olivine structure were collected from the literature (Table 1). Only those compounds were chosen for which crystal structure analyses and site refinements were available or in which cations could be assigned unambiguously to particular M-sites (*e.g.*, Mg in M1, Ca in M2 in $MgCaSiO_4$). The data set includes 31 silicates, 4

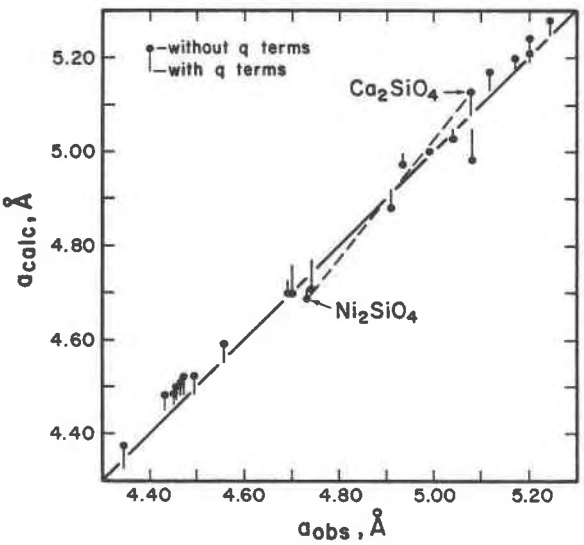

Fig. 2. A plot of a_{obs} versus a_{calc} using equations in Table 2. The data for the 31 silicate olivines were used in the regression analysis but were not plotted, except for Ni_2SiO_4 and Ca_2SiO_4, which have the lowest and highest values of a_{obs}, respectively. A dashed line connecting these two points shows the general trend for silicate olivines.

phosphates, 6 germanates, 7 beryllates, 1 borate and 3 germano-silicates.

The parameters r_{M1}, r_{M2}, and r_T refer to the Shannon (1976) effective ionic radii of the atoms occupying the M1, M2, and T sites, respectively. The formal charges of cations on M1 and M2 are designated q_{M1} and q_{M2}, respectively. The charge on the T cation has not been specified in Table 1, since $q_{M1} + q_{M2} + q_T = 8$. Using the SPSS (Nie *et al.*, 1975) multiple linear regression program, equations were calculated for a, b, c, and V; each as a function of r_{M1}, r_{M2}, r_T, q_{M1}, and q_{M2}. Results, including standard deviations (SD), F-values, and multiple coefficients of determination (R^2), are given in Table 2. Individual data sets were obtained for the silicate, phosphate, and beryllate olivines (Tables 3–5) in which a, b, c, and V were calculated as a function of r_{M1} and r_{M2} only.

Analysis of the composite data set

Based on the data set in Table 1, two multiple regression equations have been calculated for each lattice parameter: the first of each pair listed in Table 3 was determined *without* the formal charge terms, q_{M1} and q_{M2}; the second involves both charge terms. Notice that for all the equations, coefficients of determination, R^2, range from 0.970 for a to 0.997 for V, indicating that nearly all of the variation in lattice parameters can be attributed to changes in the radii of the cations. To avoid repetition in the discussion below, it should be noted that in all the regression analyses, all three radius terms, r_{M1}, r_{M2} and r_T, have significance levels (based on |t| tests) greater than 99.95%. Variation of the formal charges on the cations, however, gives statistically significant improvement only to the a parameter, as judged by the increased value of F (Dixon, 1973), although |t| tests for individual q_{M1} and q_{M2} terms are >90% for a, b, c, but not for volume.

The a cell dimension

Individual F values and coefficients for terms in the regression equations for a show that it is most highly correlated with r_{M1} and r_T, as expected from our earlier discussion of the structure (see Fig. 1). Inclusion of the charge terms in the regression equation for a results in notable improvement: the overall standard deviation decreases from 0.036 to 0.022, R^2 increases from 0.970 to 0.989, and F increases from 523 to 844. The improvement in calculated values of a is shown in Figure 2, where the data points fall considerably closer to the 45° line when q terms are included. Individual significance levels for the q terms are >99.95% for q_{M1} and 97.1% for q_{M2}, suggesting that most of the improvement in a is due to q_{M1} alone. This was confirmed in a stepwise regression analysis where, with radius terms and q_{M1} in the equation, SD = 0.023, R^2 = 0.988, and F = 969.

The b cell dimension

In contrast to a, the b cell dimension is most highly dependent on the size of the M2 cation, as predicted. The coefficient B is 5 to 7 times greater

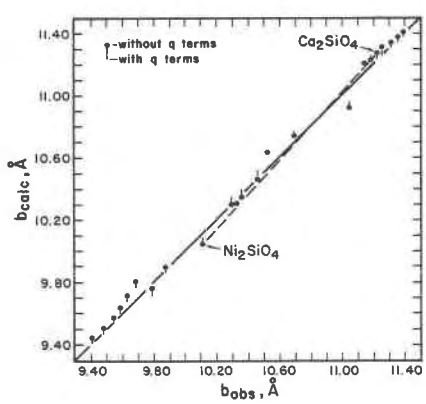

Fig. 3. A plot of b_{obs} versus b_{calc}, using equations given in Table 2. Dashed line as in Figure 2.

Table 2. Multiple regression data for 52 olivines (those *not* marked with an asterisk in Table 1). For the definition and usage of F, see Dixon (1973). To determine |t| for any term of these equations, divide the regression coefficient B by its standard error, SD.*

Dependent Variable		Independent Variables r_{M1}	r_{M2}	r_T	q_{M1}	q_{M2}	Constant	SD	R^2	F
a	B	1.096	0.330	1.105			3.419	0.036	0.970	523
	SD	0.059	0.053	0.093			0.036			
	F	343	39	142			8864			
a	B	0.915	0.277	1.303	-0.007	-0.002	3.729	0.022	0.989	844
	SD	0.043	0.034	0.062	0.001	0.001	0.051			
	F	460	65	441	80	5	5323			
b	B	0.662	3.305	0.982			7.061	0.056	0.990	1566
	SD	0.092	0.083	0.144			0.056			
	F	52	1600	46			15633			
b	B	0.468	3.231	1.193	-0.006	-0.005	7.436	0.050	0.992	1206
	SD	0.095	0.076	0.138	0.002	0.002	0.114			
	F	24	1785	74	13	5	4249			
c	B	1.045	1.623	0.651			3.859	0.034	0.991	1731
	SD	0.056	0.050	0.088			0.034			
	F	349	1044	55			12644			
c	B	1.059	1.607	0.635	0.002	-0.003	3.887	0.032	0.992	1193
	SD	0.061	0.049	0.089	0.001	0.001	0.073			
	F	300	1071	51	3	4	2816			
V	B	142.7	197.7	147.9			4.703	2.755	0.997	4631
	SD	4.5	4.0	7.0			2.758			
	F	1007	2399	441			3			
V	B	141.4	197.4	149.3	-0.057	0.006	6.480	2.802	0.997	2686
	SD	5.4	4.3	7.8	0.094	0.120	6.413			
	F	698	2108	368	0.4	0.003	1			

* For equations *with* q terms the following olivines were found to have values lying outside ±2SD (given in parentheses for each cell parameter): LiYSi, $LiFe_{0.76}Mn_{0.24}P$, MgCaGe for a (±0.044 Å); LiYSi, LiSCSi, $NaMn_{0.93}Fe_{0.07}P$ for b (±0.100 Å); CdCdGe, MnMnGe, MgCaGe for c (±0.064 Å); and MnMnGe, $NaMn_{0.93}Fe_{0.07}P$ for V (±5.6 Å^3).

If q terms are not considered in the regression equations, 2SD outliers are: LiYSi, LiYGe for a (±0.072 Å); LiYSi, LiScSi, $NaMn_{0.93}Fe_{0.07}P$, AlFeBe for b (±0.112 Å); CdCdGe, MgCaGe for c (±0.068 Å); and MnMnGe, $NaMn_{0.93}Fe_{0.07}P$ for V (±5.5 Å^3). The germanate olivines are clearly suspect, with 50% or more of the total used in the regression analyses having 2SD outliers for one or more of the lattice parameters.

for M2 than for M1 and 3 times greater than for T. As seen in Table 2, the addition of charge terms to the equation for b causes only a slight improvement in SD and R^2 but a decrease in overall F-value. Most of the data points in Figure 3 appear to fall closer to the 45° line when q terms are included in the calculation of b.

The c cell dimension

Confirming our earlier estimate, the c dimension is found to be largely a function of r_{M1} and r_{M2}. Almost no improvement is made in the equation for c by the inclusion of q terms, as seen in the plot of c_{obs} *vs.* c_{calc} (Fig. 4), where only a few of the points are brought appreciably closer to the 45° line. Contrary to our tenuous prediction, c is not correlated with the charge terms. In general, the radius

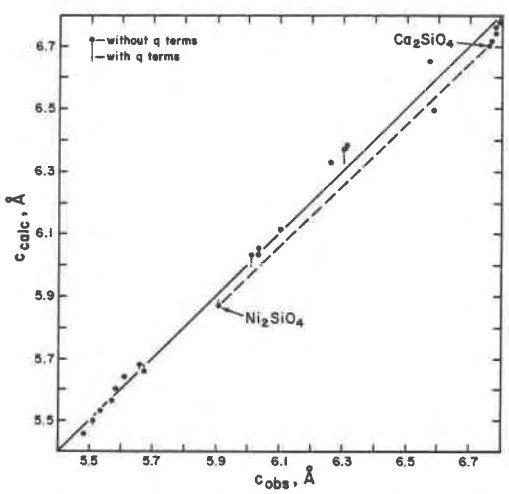

Fig. 4. A plot of c_{obs} versus c_{calc}, using equations for c_{calc} given in Table 2. Dashed line as in Figures 2 and 3.

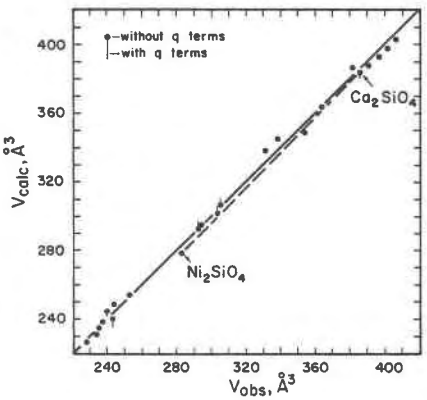

Fig. 5. A plot of V_{obs} versus V_{calc}, using equations for V_{calc} from Table 2. Dashed line as in Figures 2, 3 and 4.

terms so dominate all these regression analyses that it is obvious that cation-cation repulsion effects are largely absorbed in them.

The effects of r_{M2} on b and c may be summarized for these hexagonal closest packed olivine structures in the following terms with reference to Figures 1a and 1c: as r_{M2} increases the M2 octahedron expands between the M1–T slabs in a direction parallel to b, and it is an integral part of the edge-sharing M1–M2 and corner-sharing M2–T chains parallel to c.

The unit cell volume

As expected, the cell volume of olivine-type structures is related to the radii of all three interstitial cations, especially r_{M2} which has large contributions to b and c. Unlike the ordered silicate pyroxenes (Ribbe and Prunier, 1977), charge terms are not significant in the multiple regression equations for volume, being rejected at significance levels of 46% for q_{M1} and 5% for q_{M2} (Fig. 5).

Table 4. Multiple regression data for beryllate olivines (N = 7)

Dependent Variable		Independent Variables r_{M1}	Independent Variables r_{M2}	Constant	SD	R^2	F
a	B	1.050	0.475	3.616	0.008	0.975	78
	SD	0.116	0.086	0.069			
	F	82	31	2752			
b	B	2.271	2.449	6.890	0.009	0.997	611
	SD	0.135	0.100	0.080			
	F	282	595	7335			
c	B	1.111	1.186	4.251	0.005	0.996	475
	SD	0.075	0.055	0.044			
	F	222	459	9194			
V	B	163.5	135.8	68.5	0.613	0.996	511
	SD	9.1	6.8	5.4			
	F	322	402	159			

Analysis of individual data sets

In order to obtain more precise equations for prediction of lattice parameters, multiple regression analyses were performed separately for the $M1^{1+}$ $M2^{2+}$-phosphate, $M1^{3+}M2^{3+}$-beryllate and $M1^{2+}$ $M2^{2+}$-silicate olivines. Equations and statistics for lattice parameters versus r_{M1} and r_{M2} are given in Tables 3-5.

Phosphate olivines

As discussed below, all Li^{1+}- and Na^{1+}-containing phosphate olivines are predicted to have their monovalent cations located at M1 with divalent cations located at the M2 sites, in agreement with all known crystal structure analyses. For this reason we have taken the liberty of combining the four phosphates whose structures are not known (* in Table 1) together with the four structurally refined samples and carrying out regression analyses of cell parameters versus r_{M1} and r_{M2}. Results are given in Table 3. The R^2 values are >0.99 and standard deviations are less than approximately 0.3% of the lattice parameters. The values of SD = 0.845Å^3 and R^2 = 0.999 for the unit cell volume are outstanding.

Table 3. Multiple regression data for phosphate olivines (N = 8)

Dependent Variable		Independent Variables r_{M1}	Independent Variables r_{M2}	Constant	SD	R^2	F
a	B	1.008	0.457	3.587	0.013	0.995	495
	SD	0.059	0.088	0.047			
	F	290	27	5751			
b	B	0.202	2.864	7.927	0.022	0.995	455
	SD	0.102	0.152	0.082			
	F	4	353	9410			
c	B	0.822	1.752	4.008	0.019	0.995	465
	SD	0.091	0.136	0.073			
	F	82	166	3033			
V	B	115.1	201.3	47.2	0.845	0.999	3863
	SD	4.0	5.9	3.2			
	F	850	1169	224			

Table 5. Multiple regression data for silicate olivines (N = 29)

Dependent Variable		Independent Variable r_{M1}	Independent Variable r_{M2}	Constant	SD	R^2	F
a	B	0.932	0.236	3.918	0.010	0.982	692
	SD	0.036	0.020	0.025			
	F	659	155	24655			
b	B	0.505	3.211	7.535	0.025	0.996	3281
	SD	0.089	0.046	0.061			
	F	33	4833	15320			
c	B	1.231	1.484	4.010	0.019	0.993	1747
	SD	0.068	0.035	0.047			
	F	330	1762	7406			
V	B	149.4	187.6	46.8	1.643	0.997	3806
	SD	5.7	3.0	4.0			
	F	675	3915	140			

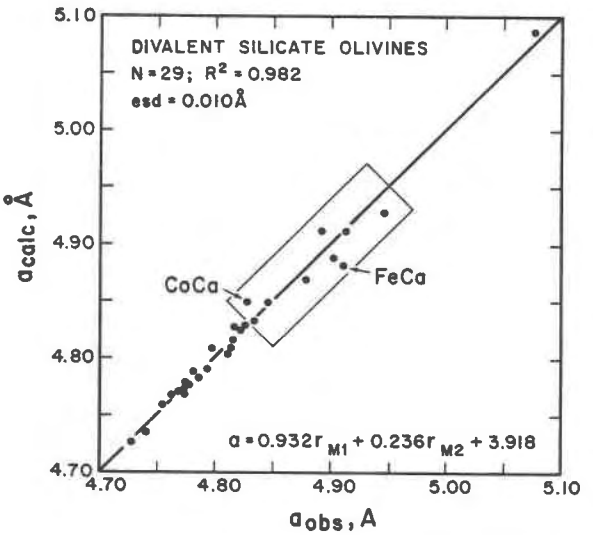

Fig. 6. A plot of observed values of the a cell dimension versus values of a calculated from the regression equation in terms of r_{M1} and r_{M2} (lower right) for the divalent silicate olivines. Labeled points are those outside the ±2SD limits. Ordered MCa olivines are bounded by the rectangle. The highest point is γ-Ca_2SiO_4.

These results appear to confirm the validity of an ordered model with M^{1+} on M1, regardless of the size of M^{2+}, at least for the size difference ($r_{M^{1+}} - r_{M^{2+}}$) observed so far (which ranges from 0.07 to −0.07Å for M^{1+} = Li and from 0.19 to −0.07Å for M^{1+} = Na). The rationalization for this is based on Pauling's (1929) third rule and follows similar arguments made by Blasse and Bril (1967) and Moore (1972): *cf.* principle (3) above. Summarizing briefly, the higher degree of edge sharing, and the short M1 · · · T distance in the M1–T slabs of the olivine structure (Fig. 1) are expected to lead to increased cationic repulsion and relative destabilization if the more highly charged of two octahedral cations occupies the M1 site. The comparatively open space between the M1-T slabs allows the M2 site to effectively handle highly charged cations. The one obvious exception, sinhalite, $Al^{M1}Mg^{M2}BO_4$, is discussed in Footnote 1 above.

Beryllate olivines

Regression data for seven beryllate olivines are presented in Table 4. The R^2 values indicate that 97.5, 99.7, 99.6, and 99.6% of the variation in a, b, c, and V, respectively, can be attributed to variation in r_{M1} and r_{M2}. Standard deviations are on the order of 0.3% for V, 0.2% for a, and 0.1% for b and c. Based on these results, the equations in Table 4 should give very accurate estimates of lattice parameters for beryllate olivines if the chemistry and ordering schemes are known or of the mean values of r_{M1} and r_{M2}, if the lattice parameters are accurately determined.

Silicate olivines with divalent octahedral cations

Because of the paucity of accurate data for M^{1+} M^{3+} silicate olivines, only those olivines with divalent octahedral cations were included in the data set. Values of R^2 ranging from 0.982 to 0.997 and standard deviations on the order of 0.5% or less (Table 5) indicate that the lattice parameters of these olivines can be adequately modelled as a linear function of the radii of the octahedral cations. (In plots of observed versus calculated lattice parameters (Figs. 6–9) no more than two 2SD outliers were found in each case, and these are specifically identified.)

An interesting feature in Figure 6 is the wide gap between ordered MCa olivines (data points enclosed in a rectangle) and Ca_2SiO_4 (the datum in the upper right corner). This is the result of the relatively strong dependence of a on r_{M1} (Table 5) and the fact that Ca in these structures is exclusively on M2. The opposite trend is shown in Figure 7 for the b cell edge, because b is strongly dependent on r_{M2}, and one Ca atom in *all* of the MCa olivines (including $CaCaSiO_4$, of course) is located in M2. These observations explain why the ordered MCa olivines have relatively low values of a and high values of b as noticed by Ganguli (1977, his Figs. 1 and 2). Although c and V are slightly more dependent on r_{M2} than r_{M1}, the effect is not great enough to

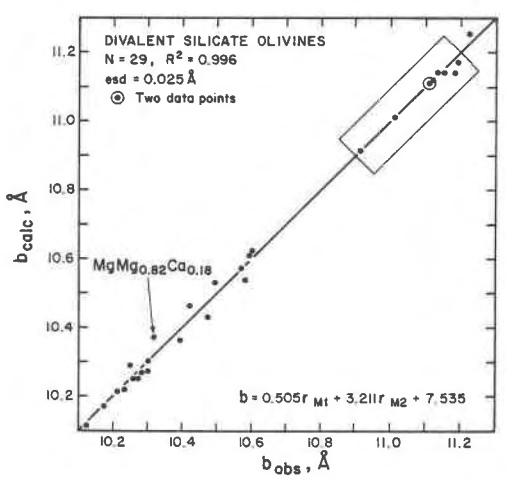

Fig. 7. A plot of b_{obs} versus b_{calc} for the divalent silicate olivines. See legend of Figure 6 for other details.

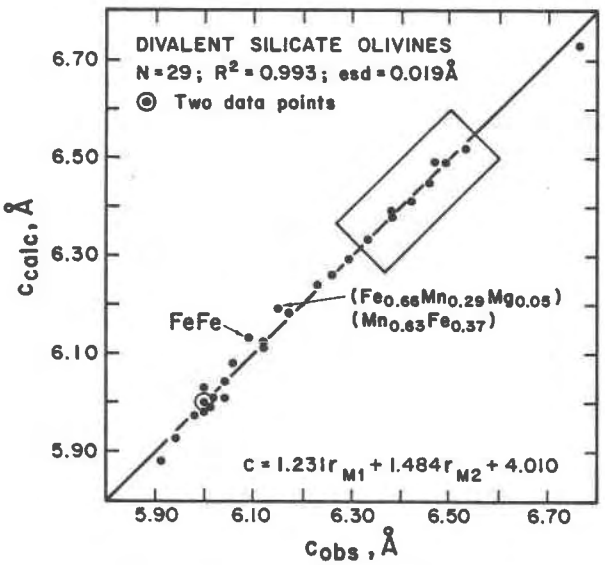

Fig. 8. A plot of c_{obs} versus c_{calc} for the divalent silicate olivines. See legend of Figure 6 for other details.

completely shift the field of ordered MCa olivines toward Ca_2SiO_4 in Figures 8 and 9.

Predictions of ordering

Because the unit cell volume is insensitive to charge effects, we have used the equation for volume *without* q terms (Table 1) in an attempt to calculate the state of cation order, disorder or antiorder of the several synthetic olivines which were *not* used in the regression analyses (marked * in Table 1). This is shown in Figure 10.

Recall that an *ordered* distribution of cations in olivine is defined as one in which the larger cation is entirely in M2 (principle 2a) and an *antiordered* distribution is defined as one in which the larger cation is in the M1 site (principle 3), regardless of the formal charges of the cations. Unfortunately, the questioned accuracy of some of the published lattice parameters (especially those for germanate olivines—see Footnote to Table 2), somewhat clouds the conclusions that can be drawn.

Germanates

Of the four germanate olivines with divalent cations, $MgMnGeO_4$, $CoMnGeO_4$, and $FeMnGeO_4$ have V_{calc} values lying closer to their observed volumes when a disordered model is used (see Fig. 10 and *cf.* Table 1). Comparing these predictions with observations of silicate olivines, a synthetic crystal of $Mg_{1.06}Mn_{0.94}SiO_4$ was found to be partially ordered with $Mg_{.72}Mn_{.28}$ in M1 and $Mg_{.34}Mn_{.66}$ in M2 (Ghose and Weidner, 1974) and a metamorphic specimen of nearly the same composition—$Mg_{1.03}Mn_{.96}(Ca,Fe)_{.01}SiO_4$—was found to be highly ordered with $Mg_{.92}Mn_{.08}$ in M1 and $Mg_{.11}Mn_{.89}$ in M2 (Francis and Ribbe, 1980). Clearly the degree of Mn/Mg order is dependent on the thermal history of these compounds, and certain quenched synthetic specimens may be expected to approach complete disorder be they silicate or germanate olivines.

As a check on the site occupancy of synthetic $MgMnGeO_4$, an *ab* plot similar to that of Figure 11 was drawn for the Mg_2GeO_4–Mn_2GeO_4 system, and it was found to be only slightly ordered (approximately $Mg_{.6}Mn_{.4}$ in M1), in close agreement with the estimate of disorder from Figure 10.

Brown (1970) found that a natural knebelite of composition $Fe_{1.03}Mn_{0.92}Mg_{0.05}SiO_4$ is partially ordered with $Fe_{.66}Mn_{.29}Mg_{.05}$ in M1 and $Fe_{.37}Mn_{.63}$ in M2. In view of this and the relatively small size difference of 0.05Å between Fe and Mn, the predicted disordered arrangement seems reasonable for a *synthetic* germanate of composition $FeMnGeO_4$.

The prediction of an ordered distribution in $ZnMnGeO_4$ (Fig. 10) is in agreement with the crystal structure determination for this sample (Lyutin *et al.*, 1974). This is consistent with the structure of a natural Mn–Mg–Zn silicate olivine (Brown, 1970) which Francis and Ribbe (1980) reinterpreted to be "fully" ordered with Mn in M2 and $Mg_{.34}Mn_{.30}Zn_{.23}Fe_{.13}$ in M1. However, it is peculiar that the unit cell volume of $ZnMnGeO_4$ is 12Å^3 larger than that of $CoMnGeO_4$ (Table 1) when the differ-

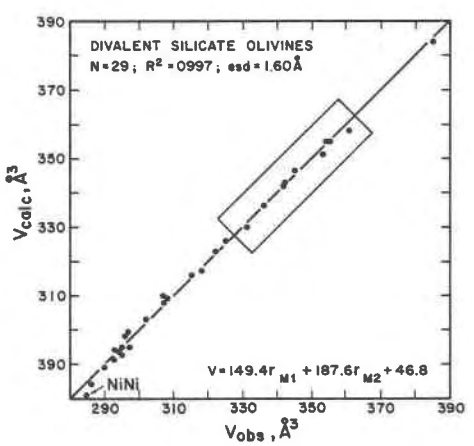

Fig. 9. A plot of V_{obs} versus V_{calc} for the divalent silicate olivines. See legend of Figure 6 for other details.

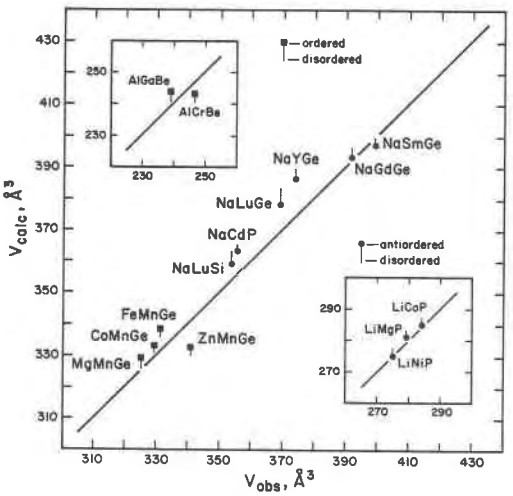

Fig. 10. A plot of the observed volume, V_{obs}, versus that calculated from the equation for V in Table 2 which does not involve q terms. Values for ordered, disordered and/or antiordered distributions of the octahedral cations (see keys) are shown for the compounds whose site occupancies were uncertain, as indicated by an asterisk * in the last column of Table 1.

ence in effective ionic radius between six-coordinated Zn and Co is only 0.005Å. No explanation for this phenomenon is immediately obvious.

Antiordered phosphates, silicates and germanates

Using Figure 10, the $M^{1+}M^{2+}$ phosphates and $M^{1+}M^{3+}$ silicate and germanate olivines with $r_{M^{1+}} > r_{M^{2+}}, r_{M^{3+}}$ are predicted to be antiordered. This prediction is borne out by crystal structure refinements of $LiScSiO_4$ (Steele *et al.*, 1978), $NaCdPO_4$ (Ivanov *et al.*, 1974), and $NaMn_{.93}Fe_{.07}PO_4$ (Moore, 1972), in all of which the larger monovalent cations are found to be on the M1 site. Kharakh *et al.* (1971) obtained the same result for $NaSmGeO_4$, which is slightly below the 45° line in our Figure 10. Additional evidence for antiordering was provided by Blasse and Bril (1967), who measured the spectral energy distribution of Eu^{3+}-doped rare earth germanates and silicates similar to those plotted in Figure 10 and concluded that Eu^{3+} cations (and therefore other REE^{3+} atoms) are located on the M2 site (principle 1).

In view of the crystal structure refinements of $Li(Fe,Mn)PO_4$ olivines in which the smaller, monovalent Li is ordered in M1 (principle 2a) (Geller and Durand, 1960; Finger and Rapp, 1970; Yakubovich *et al.*, 1978), we may predict from the lower right inset in Figure 10 that Li^+, which is slightly larger (r = 0.76Å) than Co (0.745Å), Mg (0.72Å) and Ni (0.69Å), will be "antiordered" into M1, in accordance with principle (3).

Beryllates

We are unable to draw conclusions about ordering in the two beryllate olivines (upper left inset in Fig. 10). The lattice parameters of one or both of these samples may be in error, because the unit cell volume of $AlCrBeO_4$ is reported to be 8Å^3 larger than that of $AlGaBeO_4$, although Cr^{3+} is 0.005Å smaller than Ga^{3+}. Principle (2) would suggest an ordered arrangement with Al^{3+} (r = 0.535Å) in M1 and Ga^{3+} (r = 0.62Å) in M2 in the case of $AlGaBeO_4$. On the other hand, principles (2) and (2c) are competitive in the case of $AlCrBeO_4$. Cr^{3+} is 0.08Å larger than Al^{3+} but has a d^3 electronic configuration and can gain CFSE in M1 relative to M2. By analogy with $(Fe,Mg)_2SiO_4$ olivines, we might expect $AlCrBeO_4$ to be at least partially if not completely disordered.

The $(Al,Cr)_2BeO_4$ and $(Al,Fe)_2BeO_4$ olivines studied by Newnham *et al.* (1964) are significant in this respect. Al–Cr olivines were found to be partially ordered with 60–74% (average, 68%) of the Cr^{3+} in M2. For the Al–Fe olivines, where Fe^{3+} is 0.11Å larger than Al^{3+} and can gain no CFSE (d^5 configuration), 76–91% (average, 85%) of the Fe^{3+} is located in the M2 site (see cation distributions in Table 1).

Borates

Finally, we wish to comment on ordering in synthetic $Fe^{3+}Ni^{2+}BO_4$ olivine, said to be the high pressure polymorph of the synthetic $Fe^{3+}Ni^{2+}BO_4$ compound which has the warwickite structure (Capponi *et al.*, 1973). Because Fe^{3+} (r = 0.645Å)

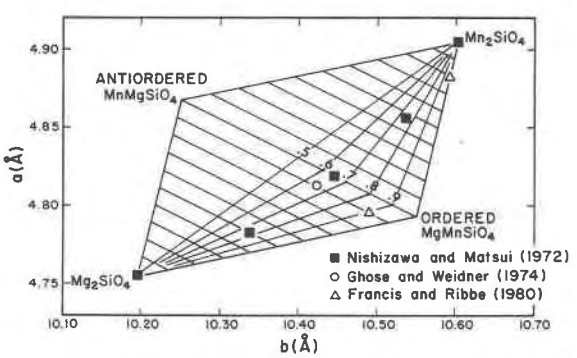

Fig. 11. An *ab* plot constructed for the Mg,Mn silicate olivines. Refer to the Appendix for method of construction and the text for details of interpretation.

and Ni^{2+} (r = 0.69Å) are of similar size, principles (2c) and (3) are expected to govern the octahedral site preference. Both CFSE (2c) and charge (3) considerations should lead to the preference of Ni^{2+} for the M1 site. However, the calculated cell volume of $Fe^{3+}Ni^{2+}BO_4$ more closely approaches the observed value of 251.1Å^3 when the larger Ni^{2+} is allocated to the M2 site (V_{calc} = 249.4Å^3) as opposed to M1 (V_{calc} = 246.8Å^3). In terms of formal valence, then, our predicted cation distribution of Fe^{3+} in M1 and Ni^{2+} in M2 agrees with the crystal structure analysis of $AlMgBO_4$ (Fang and Newnham, 1965). But unlike $AlMgBO_4$ (in which principle 2a is upheld and 3 is violated), our predicted cation distribution in $Fe^{3+}Ni^{2+}BO_4$ violates both governing principles (2c,3). Only the slightly larger size (*cf.* principle 2a) of the Ni^{2+} cation lends support to its predicted occupation of M2. Mössbauer studies might clarify the situation.

We note here that the cation distributions in the borate olivines are at odds with the refinement of a synthetic chondrodite, $Al_4Co(BO_4)_2O_2$ (Capponi and Marezio, 1975). Site occupancies of $M(1) = (Al_{0.94}Co^{2+}_{0.06})$, $M(2)$ = Al, and $M(3) = Co^{2+}_{0.89}Al_{0.11}$ were reported, where the $M(1)$ and $M(3)$ sites of this compound are geometrically analogous to the M2 and M1 sites, respectively, in olivine.

Quantitative estimates of order and composition using ab plots

An examination of the equations (without q terms) in Table 2 indicates that for the *a* cell dimension the regression coefficient for the r_{M1} term is 3.3 times greater than for the r_{M2} term; by contrast, for *b* the coefficient for the r_{M2} term is 5 times greater than that for the r_{M1} term. In the case of the silicates the ratios are closer to $B(r_{M1})/B(r_{M2}) = 4$ for *a* and 6 for *b* (Table 5). This suggests that in binary systems with a fixed value of r_T the *a* and *b* dimensions might be used to predict *quantitatively* the cation distribution in M1 and M2. Obviously, at least one condition for such utility would be a difference of ~0.1Å in the effective radii of the two octahedral cations involved.

Figure 11 has been constructed (see Appendix for details) to test this hypothesis. The *ab* plot is contoured approximately in the SW–NE direction for fractional content of Mg in the M1 site, and of the three $(Mg,Mn)_2SiO_4$ olivines whose site refinements are available (open symbols), it predicts observed contents to within 0.04 Mg/(Mg+Mn). An added benefit is that bulk composition is simultaneously determinable (NW–SE contours); predicted values are within 0.03 Mg/(Mg+Mn) for the six data points plotted within the *ab* quadrilateral.

A later paper will develop this determinative method for other natural and synthetic binary silicate olivines.

Acknowledgments

This work was supported in part by National Science Foundation grant EAR77-23114 to G. V. Gibbs and P. H. Ribbe.

References

Alberti, A. and Vezzalini, G. (1978) Madelung energies and cation distributions in olivine-type structures. Zeitschrift für Kristallographie, 147, 167–175.

Blasse, G. and Bril, A. (1976) Structure and Eu^{3+} fluorescence of lithium and sodium lanthanide silicates and germanates. Journal of Inorganic Nuclear Chemistry, 29, 2231–2241.

Brown, G. E. (1970) The Crystal Chemistry of the Olivines. Ph.D. Dissertation, Virginia Polytechnic Institute and State University, Blacksburg, Virginia.

Brown, G. E. (1980) Olivines and silicate spinels. In P. H. Ribbe, Ed., Reviews in Mineralogy, Vol. 5, Orthosilicates, p. 275–381. Mineralogical Society of America, Washington, D.C.

Capponi, J. J., Chenavas, J. and Joubert, J. C. (1973) Synthese hydrothermale a tres haute pression de deux borates de type olivine, $AlMgBO_4$ et $FeNiBO_4$. Materials Research Bulletin, 8, 275–282.

Capponi, J. J. and Marezio, M. (1975) The high-pressure synthesis and structural refinement of $Al_4Co(BO_4)_2O_2$, an anhydrous boron chondrodite. Acta Crystallographica, B31, 2440–2443.

Dixon, W. J. (Ed.) (1973) BMD, Biomedical Computer Programs. University of California Press, Berkeley, California.

Fang, J. H. and Newnham, R. E. (1965) The crystal structure of sinhalite. Mineralogical Magazine, 35, 196–199.

Finger, L. W. and Rapp, G. R. (1970) Refinement of the crystal structure of triphylite. Carnegie Institution of Washington Year Book, 68, 290–292.

Francis, C. A. and Ribbe, P. H. (1980) The forsterite–tephroite series I. Crystal structure refinements. American Mineralogist, 65, 1263–1269.

Ganguli, D. (1977) Crystal chemical aspects of olivine structures. Neues Jahrbuch für Mineralogie Abhandlungen, 130, 303–318.

Geller, S. and Durand, J. L. (1960) Refinement of the structure of $LiMnPO_4$. Acta Crystallographica, 13, 325–331.

Ghose, S., Wan, C., Okamura, F. P., Ohashi, H. and Weidner, J. R. (1975) Site preference and crystal chemistry of transition metal ions in pyroxenes and olivines. Acta Crystallographica, A31, Supplement S76.

Ghose, S. and Weidner, J. R. (1974) Site preference of transition metal ions in olivine. (abstr.) Geological Society of America Abstracts with Programs, 6, 751.

Hanke, K. (1965) Beitrage zu Kristallstrukturen vom Olivin-typ. Beitrage der Mineralogie und Petrographie, 11, 535–558.

Hill, R. J., Craig, J. R. and Gibbs, G. V. (1979) Systematics of the spinel structure type. Physics and Chemistry of Minerals, 4, 317–339.

Ivanov, Y. A., Simonov, M. A. and Belov, N. V. (1974) Crystal structure of the Na, Cd orthophosphate $NaCd[PO_4]$. Soviet Physics Crystallography, 19, 96–97.

Kamb, B. (1968) Structural basis of the olivine-spinel stability relation. American Mineralogist, 53, 1439–1455.

Kharakh, E. A., Chicagov, A. V. and Belov, N. V. (1971) Crystal structure of sodium samarium orthogermanate. Soviet Physics Crystallography, 15, 924–925.

Lyutin, V. I., Kuzman, E. A., Ilyukhin, V. V. and Belov, N. V. (1974) Crystal structure of mixed zinc-manganese orthogermanate, $ZnMnGeO_4$. Soviet Physics Doklady, 19, 10–11.

Moore, P. B. (1972) Natrophilite, $NaMn(PO_4)$, has ordered cations. American Mineralogist, 57, 1333–1344.

Nie, N. J., Hull, C. H., Jenkins, J. G., Steinbrenner, K. and Bent, D. H. (1975) Statistical Package for the Social Sciences. McGraw-Hill, New York.

Novak, G. A. and Gibbs, G. V. (1971) The crystal chemistry of the silicate garnets. American Mineralogist, 56, 791–825.

Pauling, L. (1929) The principles determining the structure of complex ionic crystals. Journal of the American Chemical Society, 51, 1010–1026.

Ribbe, P. H. (1980) The humite series and Mn-analogs. In P. H. Ribbe, Ed., Reviews in Mineralogy, Vol. 5, Orthosilicates, p. 231–274. Mineralogical Society of America, Washington, D.C.

Ribbe, P. H. and Prunier, A. R. (1977) Stereochemical systematics of ordered *C*2/*c* silicate pyroxenes. American Mineralogist, 62, 710–720.

Shannon, R. D. (1976) Revised effective ionic radii and systematic studies of interatomic distances in halides and chalcogenides. Acta Crystallographica, A32, 751–767.

Shinno, I. (1981) A Mössbauer study of ferric iron in olivine. Physics and Chemistry of Minerals, 7, 91–95.

Smith, J. V. (1966) X-ray emission microanalysis of rock-forming minerals II. Olivines. Journal of Geology, 74, 1–16.

Steele, I. M., Pluth, J. J. and Ito, J. (1978) Crystal structure of synthetic $LiScSiO_4$ olivine and comparison with isotypic Mg_2SiO_4. Zeitschrift für Kristallographie, 147, 119–127.

Sung, C. M. and Burns, R. G. (1978) Crystal structural features of the olivine → spinel transition. Physics and Chemistry of Minerals, 2, 177–197.

Virgo, D. and Hafner, S. S. (1972) Temperature-dependent Mg,Fe distribution in a lunar olivine. Earth and Planetary Science Letters, 14, 305–312.

Wenk, H.-R. and Raymond, K. N. (1973) Four new structure refinements of olivine. Zeitschrift für Kristallographie, 137, 86–105.

Yakubovich, O. V., Simonov, M. A. and Belov, N. V. (1977) The crystal structure of a synthetic triphylite $LiFe[PO_4]$. Soviet Physics Doklady, 22, 347–350.

Manuscript received, February 10, 1982;
accepted for publication, August 23, 1982.

Appendix

Construction of the *ab* plot in Figure 11:

(1) End points for Mg_2SiO_4 and Mn_2SiO_4 are from Nishizawa and Matsui (1972).

(2) The midpoint between the end-members is taken to represent disordered $MgMnSiO_4$.

(3) Equations for divalent silicate olivines (Table 5) are used to calculate *a* and *b* for both ordered and antiordered $MgMnSiO_4$.

(4) The quadrilateral is contoured for composition Mg/(Mg+Mn) at equal intervals along the line joining the Mg_2 and Mn_2 endpoints. Because data are found only in the "ordered" half, the line joining the center point (representing disordered $MgMnSiO_4$ with 0.5 Mg in M1) to the point for ordered $MgMnSiO_4$ (with 1.0 Mg in M1) has been divided into five equal segments. Thus the lower half of the quadrilateral is contoured to predict the fraction of total Mg in M1. Relative position on the *ab* plot thus yields both the bulk composition and degree of ordering of samples in the system $(Mg,Mn)_2SiO_4$.